Journal of Engineering Sciences, Assiut University, Vol. 38, No. 1, pp. 157-176, January 2010

MODELING OF THE PERMEATE FLUX DECLINE DURING MF AND UF CROSSFLOW FILTRATION OF SUGARCANE JUICE

Ali K. Abdel-Rahman
Associate Professor, Department of Mechanical Engineering,
Faculty of Engineering, Assiut University, Assiut 71516, EGYPT
E-mail: *nada_ali54@yahoo.com*

Abdel-Aziz A. Abbara
Department of Food Engineering, Al-Baath University, Homs, Syria

Mohamed R. Bayoumi
Vice President of Assiut University, Assiut, Egypt

(Received December 26, 2009 Accepted January 28, 2010)

Experimental results on permeate flux decline with time obtained from crossflow microfiltration (MF) and ultrafiltration (UF) tests were compared with those predicted numerically using the two-dimensional convective-diffusion equation. Numerical simulations of the flow and heat transfer were made using the two-dimensional momentum and energy equations. Feed solution consisted of sugarcane clear juice and limed mixed juice to pH of 7.5. Experimental tests were performed in plate and frame module employing three different MF and UF polysulphone membranes (i.e. 1 μm pore size, 25 and 100 kD molecular weight cut-off, MWCO). Influence of process variables viz. transmembrane pressure (TMP) (i.e. 1.0, 1.5 and 2.0 bar) and feed temperature (i.e. 50, 60 and 70 ^{o}C) on the flux of permeate were studied.

The present study shows that the permeate flux obtained both experimentally and numerically is increased as the transmembrane pressure is increased for all the membranes considered in this study. Moreover, permeate flux has been increased as the feed temperature is increased and decreased with time. Numerical predictions of permeate flux show a reasonable agreement with experimental counterparts.

KEYWORDS: *Flux decline, Numerical modeling, Microfiltration, Ultrafiltration, Transmembrane pressure.*

1. INTRODUCTION

Crossflow membrane UF and MF have been considered as two promising technologies to solve many separation problems in various industries such as chemical and food industries. The purification of sugarcane juice by membrane filtration promises a significant improvement in the sugar quality and yield [1]. Madsen *et al*. [2] suggested that it should be possible to introduce membrane filtration as a unit operation in the sugar industry. However, the growth of the technologies, especially for MF and UF, has fallen far behind the initial anticipation. One of the major obstacles which hinder more widespread application of UF and MF is that the permeate flux declines with time (commonly named fouling) [3].

NOMENCLATURE

Alphabetic Symbols

c	concentration (kg /kg)	u	mean streamwise velocity (m/s)
c_w	concentration near membrane wall (kg /kg)	v	velocity in y direction (m/s)
		v_w	wall velocity (m/s)
c_o	feed concentration (kg /kg)	v_{wo}	wall velocity at the beginning of permeation (m/s)
c_p	specific heat capacity (kJ/kg K)		
D	Diffusion coefficient (m^2/s)	x	Cartesian coordinate in the streamwise direction
f	rejection of the membrane		
h	channel half-width (m)	y	Cartesian coordinate normal to the wall
k_t	thermal conductivity (W/m K)		
L	channel length (m)	*Greek Symbols*	
P	pressure (Pa)	β	constant in Eq. (8)
S_Φ	source term of the variable ϕ	ΔV	cell volume (m^3)
S_p	coefficient in the discretized source term	ϕ	any of variables to be solved
		Γ_Φ	diffusion coefficient of the variable ϕ
S_u	coefficient in the discretized source term	μ	dynamic viscosity (Pa .s)
t	time (s)	ρ	density (kg/m^3)
T	temperature (^oC)		

Membrane fouling is a very complicated phenomenon mainly caused by adsorption of particles, pore shrinkage and blockage; deposition of particles on the membrane surface and concentration polarization. A number of mathematical models [4-8] are available in the literature that attempt to describe the mechanism of transport of particles through membranes such as Brownian diffusion, inertial lift, shear-induced diffusion, flowing cake and surface transport, and cake layer models. The resistance-in-series model is used frequently, in which permeation flux declines due to membrane fouling and concentration polarization resistance on the membrane surface [9,10]. Many researchers thought that the formation of cake layer was the main reason, which resulted in unsteady-state transient flux decline in cross-flow microfiltration [11-14].

Furukawa *et al*. [15] proposed a modified analytical method incorporated with the concept of dead-end filtration to determine the initial flux of crossflow filtration. The modified analysis provided an accurate prediction of permeate flux during the filtration of soy sauce lees. Shengji *et al*. [16] proposed a mathematical model to predict the membrane flux using the raw water quality (turbidity), TMP and temperature as parameters. The results showed that the model can well predict the membrane flux. Wang *et al*. [17] have developed a simple convective model for unsteady-state transient flux in crossflow microfiltration based on the assumption that the variation rate of average thickness of the deposition layer is proportional to the difference in the masses of solutes brought to the membrane surface by the bulk fluid flow and the solutes removed from the membrane surface by the shear rate of the tangential flow.

These models suffer from the improper assumptions used and oversimplifications. Cake filtration model, as an example, is not appropriate for application to crossflow filtration where the feed solution continuously recirculates.

Furthermore, macromolecules and/or colloidal particles experience diffusion which is not considered in this model. Moreover, the concentration polarization model is inherently weak in describing two-dimensional mass transport mechanisms during crossflow filtration. Also, it results in the well-known flux paradox problem: the predicted permeate flux can be much less than that measured during filtration of colloidal suspensions [18].

Recently, many attempts have been made to fully describe the two-dimensional mass transport mechanisms involved in crossflow filtration. Several authors have tried to solve the differential equation numerically in order to obtain the concentration profiles inside the membrane channel; most of these efforts were limited to the steady-state case [19,20] and some were directed towards the unsteady-state case [21,22]. Pak *et al*. [23] simulated numerically the laminar fluid flow in porous tubes of crossflow filtration tubular membrane using the computational fluid dynamics (CFD) techniques. A two dimensional numerical solution of the coupled Navier-Stokes, Darcy's law and mass transfer equation has been developed using control volume based finite difference method. Predictions of the growth rate of the concentration polarization boundary layer along the length of tubular membrane have been performed.

Although the concentration profiles can explain the trends in flux decline, they cannot be directly used to predict the flux decline. Therefore, it was found necessary to develop a comprehensive model which can predict the flux decline during crossflow filtration. Lee and Clark [18] have mathematically expressed the mass transfer during crossflow ultrafiltration using the two-dimensional convective-diffusion equation. A step-wise pseudo steady-state model was developed to predict the flux decline due to concentration polarization during crossflow ultrafiltration. Their results showed that the step-wise pseudo steady-state model predictions were in good agreement with experimental results of flux decline during crossflow ultrafiltration of colloidal suspensions.

Computational fluid dynamics, together with mass transfer modeling, have been proved to be a powerful tool to be used in the feed-side of membrane modules to facilitate the predictions of permeate flux [18]. One or more of the following simplifications had been made in the previous studies: (a) the fluid flow field was approximated by some prescribed functions or by a reduced form of the momentum equation; (b) effect of axial pressure drop on wall velocity was neglected or an approximate pressure drop was used without solving the momentum equation; and (c) the fluid transport properties were assumed constant or concentration-dependent viscosity and diffusion coefficient were used.

This study is carried out to investigate, both experimentally and numerically, the performance of a plate and frame membrane module for the MF and UF of sugarcane juice. The effect of membrane type, TMP and the feed temperature on the permeate flux is analyzed. Moreover, the present study is directed towards establishing a numerical method capable of predicting the permeate flux decline taking into account the variable properties of the stream. For this purpose, the unsteady-state full Navier-Stokes equations along with the mass and energy transfer equations are solved using a finite volume discrete scheme which employ the SIMPLE (Semi-Implicit Method for Pressure Linked Equations) pressure-correction scheme combined with QUICK

(Quadratic Upwind Interpolation Convective Kinematics) scheme in the frame of staggered grid.

2. MODEL PROBLEM AND DISCRETIZATION

2.1 Governing Equations

In crossflow membrane filtration the feed stream, which flows mainly tangentially to the porous membrane surface, is modeled by the Navier-Stokes, mass and energy transfer equations by the two dimensional convective and diffusion equation.

For two dimensional, incompressible, unsteady laminar channel flows; the continuity and Navier-Stokes equations are given as [24];

$$\frac{\partial \rho}{\partial t}+\frac{\partial u}{\partial x}+\frac{\partial v}{\partial y}=0 \tag{1}$$

$$\frac{\partial(\rho u)}{\partial t}+\frac{\partial(\rho u u)}{\partial x}+\frac{\partial(\rho\, vu)}{\partial y}-\frac{\partial}{\partial x}[\mu(\frac{\partial u}{\partial x})]-\frac{\partial}{\partial y}[\mu(\frac{\partial u}{\partial y})]+\frac{\partial P}{\partial x}=0 \tag{2}$$

$$\frac{\partial(\rho v)}{\partial t}+\frac{\partial(\rho u v)}{\partial x}+\frac{\partial(\rho\, vv)}{\partial y}-\frac{\partial}{\partial x}[\mu(\frac{\partial v}{\partial x})]-\frac{\partial}{\partial y}[\mu(\frac{\partial v}{\partial y})]+\frac{\partial P}{\partial y}=0 \tag{3}$$

Where, u and v are the streamwise and transverse velocity components, respectively; P is the pressure, ρ is the density and μ is the dynamic viscosity.

Mass transfer occurring within domains with porous walls can be mathematically expressed by the two dimensional convective and diffusion equation as follows [24];

$$\frac{\partial(\rho c)}{\partial t}+\frac{\partial(\rho uc)}{\partial x}+\frac{\partial(\rho\, vc)}{\partial y}-\frac{\partial}{\partial x}[D(\frac{\partial c}{\partial x})]-\frac{\partial}{\partial y}[D(\frac{\partial c}{\partial y})]=0 \tag{4}$$

Where D is the solute diffusion coefficient and c is the solute concentration.

Most of the previous models solve equations (1)-(4) using constant or concentration-dependent only thermophysical and flow properties. In the present study, the energy equation has to be solved to account for the temperature dependence of the abovementioned properties. For two dimensional, incompressible, unsteady laminar channel flows; the energy equation is given as [24]

$$\frac{\partial(\rho T)}{\partial t}+\frac{\partial(\rho uT)}{\partial x}+\frac{\partial(\rho vT)}{\partial y}-\frac{\partial}{\partial x}[\frac{k_t}{c_p}(\frac{\partial T}{\partial x})]-\frac{\partial}{\partial y}[\frac{k_t}{c_p}(\frac{\partial T}{\partial y})]=0 \tag{5}$$

where k_t and c_p are the fluid thermal conductivity and specific heat at constant pressure, respectively; T is the fluid temperature.

2.2 Computational Domain and Grid System

The physical problem considered in the present study is steady state laminar channel flow with permeable walls. **Figure 1** displays the flow geometry and the coordinate

system used for the problem considered. The local permeation velocity through the membrane, v_w, was specified as a function of the wall concentration of solute, c_w, as shown in Section 2.4. This leads to a more physically meaningful solution.

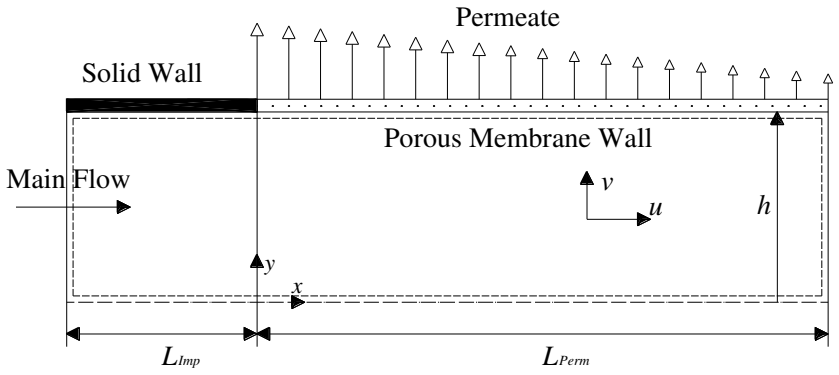

Figure 1: Schematic diagram of flow geometry and computational domain.

The computations are carried out in the rectangular domain shown in **Fig. 1**. The origin of the streamwise coordinate, x, is located at the beginning of the membrane and the origin of the normal coordinate, y, is set at the horizontal midplane of the channel. The position of the inlet section for the computational domain is located at a position L_{Imp} upstream from the starting point of the membrane, and that of the outlet section is located at a position L_{Perm} downstream from the starting point of the membrane. The main result were obtained for a computational domain of $-10 \leq x/h \leq 100$, i.e. $L_{Imp} = 10\ h$ and $L_{Perm} = 100\ h$.

One of the important points of numerical solution is the choice of grid point system for which the equations are discretised. In relation with the use of the SIMPLE scheme, a staggered grid is used in this work [21]. A nonuniform grid system was employed and the grid density was made higher near the leading edge of the membrane in x direction and near the walls in the y direction to take into accounts the steep change of velocity, temperature and concentration there. Grid points of total number of 251x100 were allocated in the computational domain. About 70 percent of the cross-stream grids were located at a distance of $0.2h$ from the membrane wall (the maximum step size in the y-direction needs to be less than or equal to $1\text{x}10^{-5}$). Numerical experiments using different sets of grids were carried out in order to prove the sufficiency of the selected grid system. The number of elements is chosen to be 25,100 (251x100) because further refinement of the mesh to 50,200 elements produced just a 0.2% difference in flux decline values. This is proved to be an important requirement for the stability of numerical procedure [20].

2.3 Discretization

The unsteady-state form of the conservation equations of continuity, momentum, concentration and energy can be written in a general form as [25];

$$\frac{\partial(\rho\phi)}{\partial t}+\frac{\partial(\rho u\phi)}{\partial x}+\frac{\partial(\rho v\phi)}{\partial y}-\frac{\partial}{\partial x}[\Gamma_\phi(\frac{\partial\phi}{\partial x})]-\frac{\partial}{\partial y}[\Gamma_\phi(\frac{\partial\phi}{\partial y})]-S_\phi=0 \quad (6)$$

where ϕ stands for any of the variables to be solved, Γ_Φ is the diffusion coefficient, and S_Φ is the source term of the variable ϕ. For $\phi = u$ *or* v *and* $\Gamma_\Phi = \mu$ one gets the momentum equations, while for $\phi = 1$ and $\Gamma_\Phi = 0$ one obtains the continuity equation [26]. If $\phi = T$ and $\Gamma_\Phi = k_t/c_p$ one gets the energy equation. When $\phi = c$ and $\Gamma_\Phi = D$, the general equation stands for the mass transfer equation [19, 27].

All the governing equations are discretized by first integrating them over a control volume (CV) and then approximating the fluxes of variable crossing every faces of each cell in term of the values at the neighboring grid points. In the present work, a QUICK scheme, which can handle uniform and non-uniform grid systems, is used to finite difference the convective terms and to secure second order accuracy in central differencing the diffusive fluxes. The resulting finite-difference equations are described in the form of [28]

$$a_p \phi_p = \sum_i a_i \phi_i + S_u \Delta V + a_p^o \phi_p^o, \qquad i=E, W, N, S, EE, WW, NN, SS, \quad (7a)$$

$$a_p = \sum_i a_i + a_p^o - S_p \Delta V, \qquad i=E, W, N, S, EE, WW, NN, SS, \quad (7b)$$

where ΔV is the cell volume, *E, W, N, S, EE, WW, NN, and SS* stand for the east, west, north, south, east of east, west of west, north of north and south of south grid points; respectively, and S_p and S_u are the coefficient appearing in the following linearized source term;

$$S_\phi = S_u + S_p \phi \quad (7c)$$

The finite difference coefficients a_i are the coefficients describing the magnitudes of the sum of the convective and diffusive fluxes and contain the geometric properties of the control volume. They are given with details in [28].

2.4 Boundary Conditions

The boundary conditions of the problem are shown in **Fig. 2**.

1- At the inlet, the flow is assumed to be fully developed thus a parabolic flow is specified. A uniform inflow concentration of c_o is specified. A constant inlet temperature T_o is specified.

2- At the symmetry plane, $v = 0$, and the normal gradients of the tangential velocity u, the concentration and temperature are set to zero.

3- At the membrane walls, the conditions are more complex, as flow permeates through the wall. For a membrane located at the plane $y = h$, a constant rejection and variable permeation rate were specified. The tangential velocity u is set to zero i.e. no slip at membrane wall, which characterizes the flows with solid bounding walls. Temperature at the membrane wall T_w was set to a constant value. Variation in permeation was modeled using the following expression proposed by Brian [29] referenced by Wiley and Fletcher [30];

$$v_w = v_{wo}[1 - \beta(\frac{c_w}{c_o} - 1)] \quad (8)$$

where v_{wo} is the wall velocity at the beginning of permeation, c_w is the concentration near membrane wall and β is constant which has the value of one for variable wall flux [30].

The boundary condition on the concentration results from a balance of the convective and diffusive fluxes. In addition, it must be taken into account the fact that not all of the solute permeates through the membrane. This is done via the use of a rejection coefficient, *f*, and the concentration boundary condition is given by;

$$D\frac{\partial c}{\partial y} + v_w\, f\, c_w = 0 \tag{9}$$

4- At the exit, both the flow, temperature and concentration fields are assumed to obey the boundary layer approximation. It is important to mention that this treatment of the down stream end boundary condition has proved to be robust and effective in shortening the computational domain leading to the reduction of the number of grid nodes [26, 28].

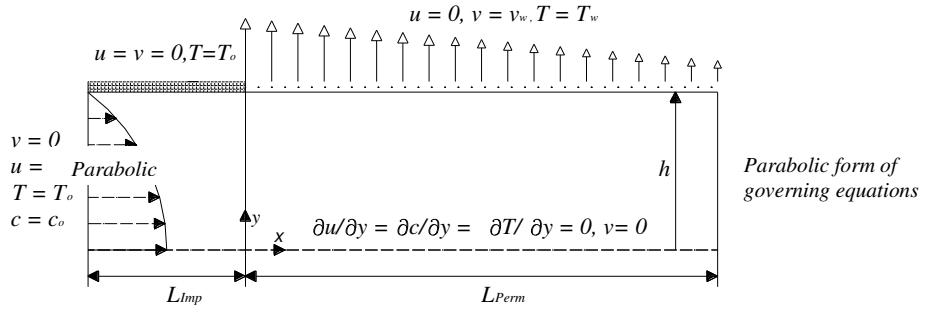

Figure 2: Boundary conditions.

2.5 Numerical procedure

The present study utilizes a modified version of the SIMPLE procedures developed by Patankar and Spalding [25]. For each time interval, the main steps of the SIMPLE algorithm are;

1- A pressure field is assumed,
2- It is used to obtain approximate velocity field,
3- The velocity and pressure fields are corrected if the former does not satisfy the continuity equation,
4- Solve the discretization equations for the other ϕ 's such as temperature and concentration providing their influence on the flow field.
5- Return to step 2 with the corrected velocity field and the new values of all other ϕ 's and then the process 2-4 are repeated until a converged solution is obtained.

In the present work, the cross-stream distribution of *u*-velocity component is adjusted to satisfy the overall continuity (conservation of the mass flow are integrated over a cross-stream line) whereas the pressure field is adjusted to satisfy the overall momentum balance. This procedure is important especially for the present problem in which the flow is changed as the flow moves downstream due to the suction of the permeate flux from the membrane surface [24, 31]. Moreover, the cross-stream distribution of the concentration is adjusted to satisfy the overall mass concentration of the permeated species.

An alternating direction implicit (ADI) procedure, which has been developed by Abdel-Rahman and Suzuki [26], has been combined with the iterative solution procedure of equations (7) to enhance isotropic propagation of a change of variables occurring at one point to the surrounding. This procedure makes use of the line-by-line Tri-Diagonal Matrix Algorithm (TDMA) solver. In the ADI procedure, sweep of line-by-line integration was carried out along both north-south grid lines and along east-west grid lines alternatively. The same procedure was applied twice for the pressure correction [28].

2.6 Physical Properties

In the present study the solvent was a pure sucrose solution with a concentration corresponding to the raw cane juice. Expressions for the variation of physical properties with temperature and concentration for sugar solution were taken from sugar technologist manual edited by Bubnik *et al.* [32].

3. EXPERIMENTAL METHODS AND MATERIALS

The main aim of this study was to investigate the permeate flux decline in MF/UF clarification of the mixed juice. A test rig was designed and constructed at Sugar Technology Research Institute, Assiut University to serve this purpose. In order to reflect the real properties of mixed juice, this research was carried out on-site at the Pilot Plant for Sugar Research at the Qus Sugar Mill.

3.1 Materials

The feed to the test rig was either the hot fresh mixed juice or the clear juice. Mixed juice was collected from the sampler tank located after the mill house at Qus factory. The clear juice was obtained by adding the milk of lime to the mixed juice at a temperature of about 72 ^{o}C under constant stirring to increase the pH to the preset value.

Four organic flat sheet membranes of different pore size or MWCO were selected in the present study. They were obtained from Alfa Laval Nakskov A/S Company, Denmark and used without any further modification. The main characteristics of these membranes are given in Abbara [33]. Pre-filters were used to remove fibrous material and suspended solids that foul the membrane.

3.2 Experimental Set-Up

The microfiltration and the ultrafiltration (MF/UF) experiments were carried out in a simple and flexible filtration system designed and assembled at the Sugar Technology Research Institute of Assiut University. The experimental set-up is shown in **Fig. 3**. Pre-filters and MF/UF module were arranged so that each component could operate alone or in series with the others. Pressure gauges were mounted at the inlet and outlet of pre-filters and the membrane module. The feed vessel and the receiving tank are equipped with stirrers of variable speeds and steam coils for heating. Level indicators and temperature sensors are also mounted.

The solution is pumped to the P-KG plastic prefilter in which an ultrapolydepth® PP-TF depth filter of 50 µm is used to remove suspended particles prior to microfiltration and ultrafiltration is installed. The solution from the prefilter is either directed to the other prefilter with element of pore size less than the first one then to the membrane module, or to the receiving vessel.

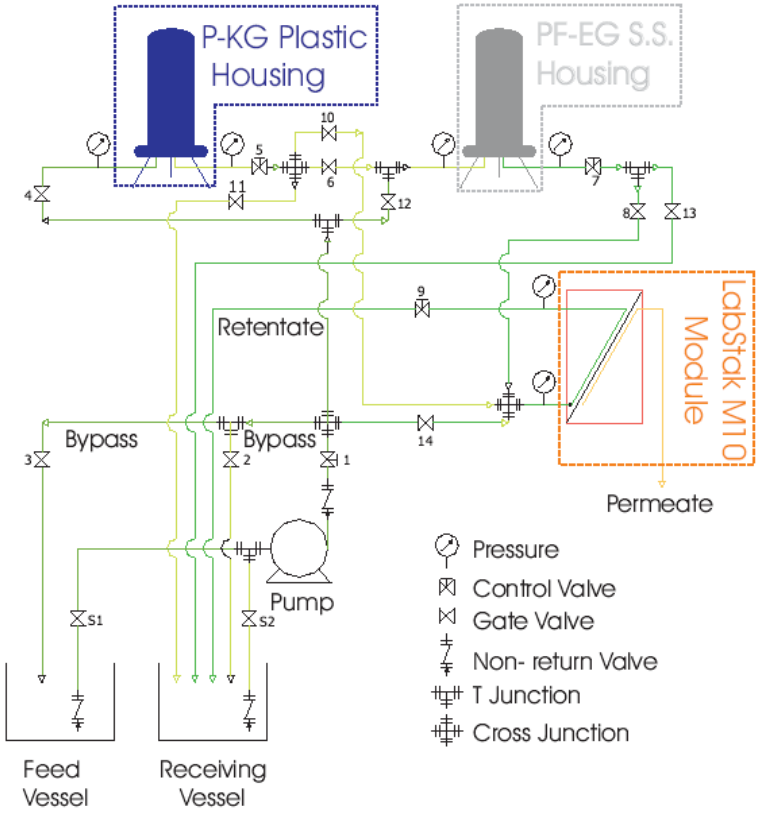

Figure 3: Schematic flow diagram of the experimental set-up

3.3 Experimental Procedure and Analysis

A group of experiments were planned to determine the membrane permeate flux decline fouling characteristics and to examine the agreement of membrane filtration with present numerical model. These experiments were carried out using three types of membrane installed simultaneously on the membrane module. The membranes were of type: GRM0.1PP MF, GR40PP and GR60PP UF. Inlet and outlet pressures are measured with pressure transducers mounted on the inlet and outlet of the membrane module. Transmembrane pressure (TMP) was calculated as the average value of inlet and outlet pressures. Juice was heated to the required temperature by a steam coil immersed in the feed vessel. The experiments were carried out at temperatures of 50, 60 and 70 ^{o}C and at different TMP of 1.0, 1.5 and 2.0 bar.

The membrane filtration was performed in a batch mode with recycling permeate and retentate back to the feed vessel to simulate the continuous operation.

Permeate flow rate was measured by collecting the permeate in a 500 ml measuring cylinder and the collection time of 50 ml of permeate is recorded. The total run time for each membrane test was 1.5 hours. After each experiment, the membrane was cleaned in place (CIP) with clean water for about one hour.

To determine the membrane fouling, the water flux was measured both before and after the cane juice membrane filtration at TMP of 0.85 bar and temperature of 60 ^{o}C. The membrane fouling was calculated as a percentage drop in the water flux.

4. RESULTS AND DISCUSSION

4.1 Effect of Operating Parameters on the Flux Behavior of Clear Juice

The effect of TMP and temperature on the permeate flux from microfiltration of the clear juice through GRM0.1PP obtained experimentally and numerically is given in Fig. 4. As shown from this figure, for TMP of 1.0 bar and solution temperature of 60^{o}C, the flux decreases rapidly from 107 (corresponding numerical value is: 108) L/m^2.h to about 88 (86.5) L/m^2.h during the first ten minutes of operation. After that, the flux was decreased slowly towards the end of the first run to stabilize around the value of 70 (70.3) L/m^2.h. The membrane fouling obtained experimentally was 69.9%. The rapid decline in flux initially could be attributed to the formation of a gel layer. Then the flux was stabilized once the dynamic equilibrium of macromolecular diffusion is established between the bulk flow and the gel membrane while the gel layer remains constant.

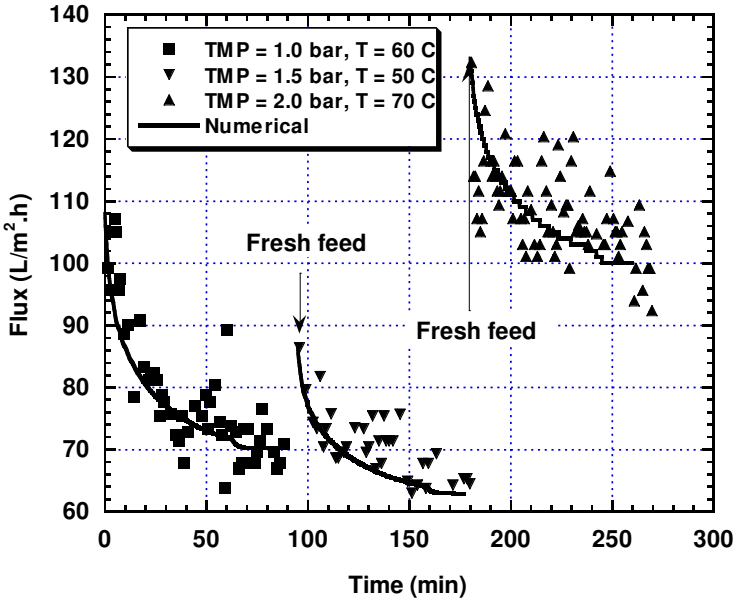

Figure 4: Effect of TMP and temperature on the permeate flux of clear juice filtered through GRM 0.1PP membrane.

Increasing the TMP to 1.5 bar with decreasing the temperature to 50^{o}C in the second run did not affect the flux and still to be around 68 (62.9) L/m^2.h towards the

end of the run. This means that decreasing the temperature offset the increase in TMP. However, increasing the TMP to 2.0 bar and the temperature to 70°C led to the increase of the flux to the maximum value of about 130 (133) L/m^2.h. Then the flux was decreased to about 92 (shortly before the end of the run: 100) L/m^2.h at the end of the run. The membrane fouling obtained experimentally was 4.3% for the third run. The decrease in the membrane fouling percentage from 69.9% to 4.3% could be attributed to the pore blockage of the membrane. The figure shows that the present numerical model is capable to predict the flux decline phenomena and the numerically obtained results agree well with its experimental counterpart.

The effect of temperature and TMP on the flux from ultrafiltration of clear juice through GR40PP and GR60PP membranes obtained experimentally and numerically is shown in Figs. 5 and 6, respectively. Figure 5 shows that, for TMP of 1.0 bar and temperature of 70°C the flux decreases rapidly from 88 (90) L/m^2.h to about 72 (76.9) L/m^2.h during the first ten minutes of operation. After that, the flux was decreased slowly towards the end of the first run to stabilize around the value of 65 (66.2) L/m^2.h. Increasing the TMP to 2.0 bar with decreasing the temperature to 50°C in the second run did not affect the flux and still to be around 60 (59.6) L/m^2.h towards the end of the run. This means that decreasing the temperature offset the increase in TMP. In the third experiment, TMP was decreased to 1.5 bar with raising the temperature to 60°C. This led to the decrease of the flux to the value of 44 (46.4) L/m^2.h at the end of the run. This decrease could be attributed to the pore blockage of the membrane and the decrease in TMP, which offset the increase in temperature. This finding is similar to that obtained in case of MF tests. Again, the figure shows that the present numerical model is capable to predict the flux decline phenomena and the numerically obtained results agree well with its experimental counterpart.

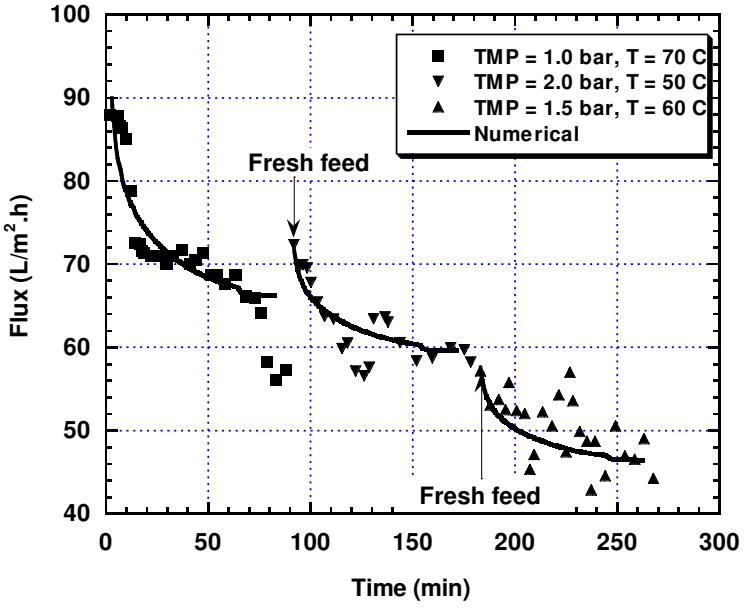

Figure 5: Effect of TMP and temperature on the permeate flux of clear juice filtered through GR40PP membrane.

The membrane fouling values of GR40PP membrane obtained experimentally in the present study are given in Table 1. Table 1 indicates that, the membrane fouling was the highest for the first experiment. This coincides with the results obtained for the MF test (GRM0.1PP membrane) where its fouling value was also found to be the highest for the first run, which can be explained as before.

Table 1: Membrane fouling for GR40PP UF at different conditions of operation

Exp.	**1**	**2**	**3**
TMP (bar)	1	2	1.5
Temperature (^{o}C)	70	50	60
Membrane Fouling %	45.2	4.92	28.9

Figure 6 shows the effect of temperature and TMP on the flux from ultrafiltration of clear juice through GR60PP membrane obtained experimentally and numerically. As it is expected, the lowest flux obtained experimentally and numerically should be at the conditions of temperature of 50^{o}C and at the TMP of 1.0 bar for the membrane GR60PP as shown in Fig. 6. Moreover, the membrane used in this experiment was first used for the first 90 minutes to filter a clear juice obtained through boiling of the mixed juice (not shown in the figure). This explains why the flux was so low. Raising both the TMP to 1.5 bar and the temperature to 70^{o}C almost double the flux. In the third experiment, the flux decreased to about 42 (39.8) L/m^{2}.h towards the end of the run. The figure shows that the numerical results obtained for permeate flux agree reasonably with the experimental one although the rate of permeate flux decline predicted numerically is higher than that obtained experimentally especially at the conditions of temperature of 50^{o}C and at the TMP of 1.0 bar. Membrane fouling values of GR60PP membrane are shown in Table 2.

Table 2: Membrane fouling for GR60PP UF at different conditions of operation

Exp.	**M.J.**	**1**	**2**	**3**
TMP (bar)	1.0	1.0	1.5	2.0
Temperature (^{o}C)	50	50	70	60
Membrane Fouling %	62.9	12.5	0.72	23.8

From Table 2, it is clear that the GR60PP membrane behavior is similar to the other membranes, i.e. the membrane fouling is the highest at the end of the first run. This could be attributed to the irreversible fouling layer composed during the filtration of the clear or mixed juice through membranes. In addition, the temperature seemed to have no profound effect on the membrane fouling.

Figures 4 to 6 show clearly that the highest flux obtained experimentally and numerically for each membrane occurs when both the temperature and the TMP are high. Moreover, the effect of feed temperature rise is more profound than the increase in the TMP. However, it was explained that the TMP and the temperature have no significant effect on the quality of permeate [33]. Therefore, it is recommended to operate the membrane at high temperature (70^{o}C) and at a moderate TMP (2.0 bar) to obtain the highest permeate flux.

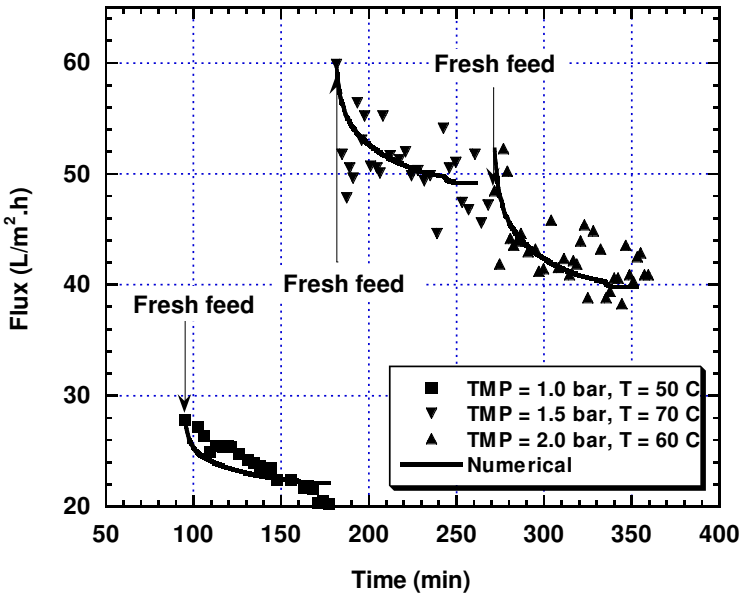

Figure 6: Effect of TMP and temperature on the permeate flux of clear juice filtered through GR60PP membrane.

4.2 Effect of Operating Parameters on the Flux Behavior of Clear Juice

In this study, two strategies were used to clarify mixed juice through GRM0.1PP, GR40PP and GR60PP membranes. First, mixed juice was boiled and left to settle for two hours and the clear juice was filtered through membranes. Second, mixed juice was filtered directly through membranes. In both cases, the mixed juice was initially filtered through prefilter (depth filter) with 50 μm. Boiling the mixed juice coagulate protein and other colloidal matter which could minimize fouling.

During the following experiments, the membrane used was old, i.e it was used for clarifying clear juice. Flux behavior obtained experimentally and numerically is shown in Figs. 7 through 9.

As shown in Fig. 7, the flux decline is almost the same between the mixed juice treated to the boiling point and mixed juice without treatment although the rate of flux decline was nearly linear for the first case. This linearity of flux decline could be attributed to the fact that boiling the mixed juice has the effect of minimizing fouling. Numerical results obtained in this study have predicted this behavior although the predicted flux is higher than the experimental one towards the end of the run. However, increasing the temperature increases the flux, almost 1.5 times.

As shown in Fig. 8, the flux decline was similar to those of clear juice, and the permeate flux is increased with increasing temperature, from about 42 (41.3) L/m^2.h to about 60 (59.9) L/m^2.h. Data shown in Fig. 9 are obtained using new membrane in both cases of boiled juice and mixed juice at a temperature of 50^{o}C and at different TMP in order to show the effect of the TMP only. Figure 9 shows that increasing the TMP increases the flux. Figure 7 also shows that the method of treatment of mixed juice has no effect on permeate flux. Hence, the observed increase in permeate flux could be

attributed mainly to the TMP solely. For the mixed juice without treatment, the figure shows that the effect of temperature is to increase the permeate flux. However, flux decline was sharp in the last experiment, which could be attributed to the heavy fouling caused by constituents of mixed juice.

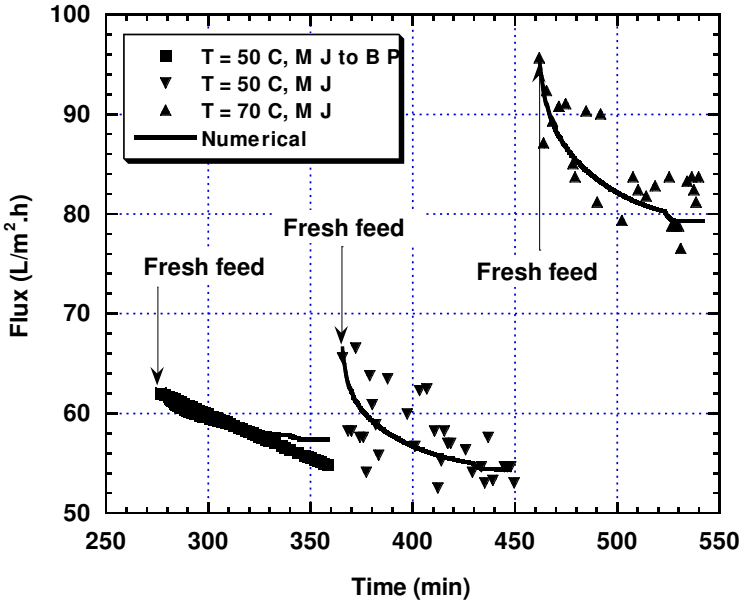

Figure 7: Effect of temperature and method of treatment on the permeate flux of mixed juice filtered through GRM0.1PP membrane at TMP of 1.5 bar.

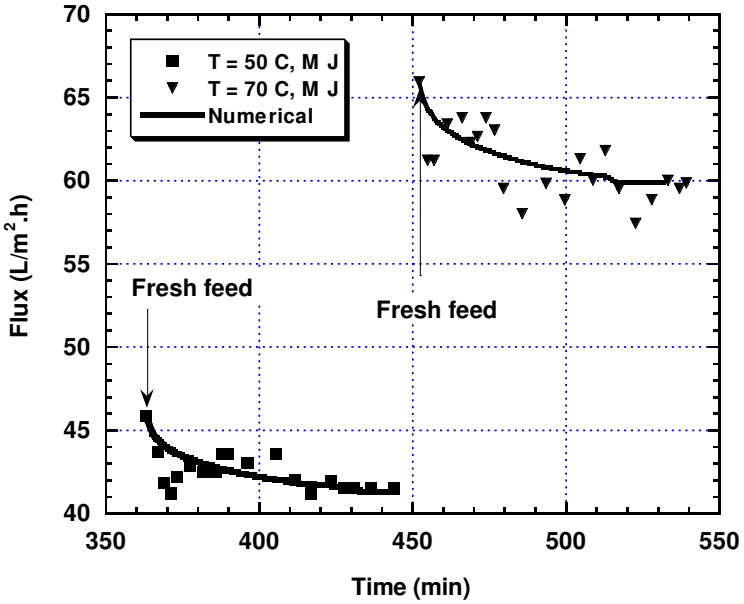

Figure 8: Effect of temperature on the permeate flux of mixed juice filtered through GR40PP membrane at TMP of 2.0 bar.

The problem of clarifying mixed juice with membrane is clogging the prefilter rapidly, so that it needs cleaning at short periods. Another problem arises from the danger of sugar inversion at the subsequent steps of white sugar production. Accordingly, it is recommended to use MF and/ or UF process on clear juice.

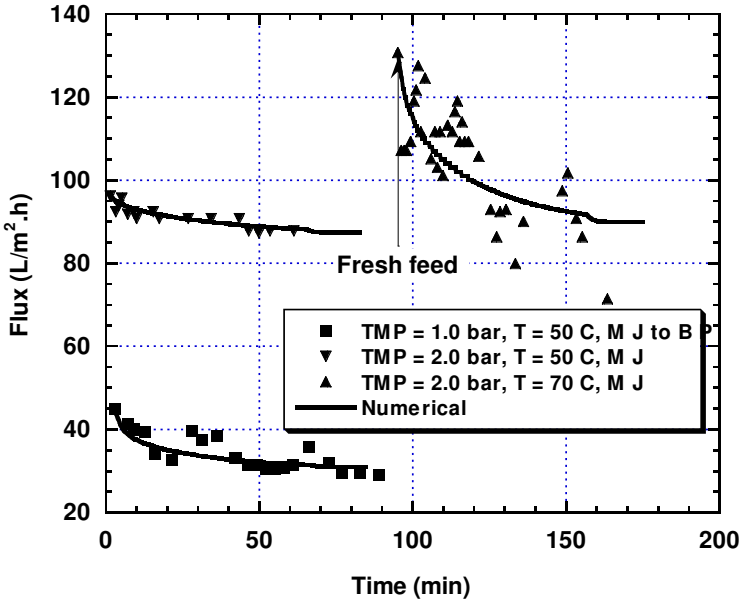

Figure 9: Effect of temperature, TMP and method of treatment on the permeate flux of mixed juice filtered through GR60PP membrane.

4.3 Effect of Operating Time on the Flux Behavior

To shed light on the performance of membrane separation process, the present study examines experimentally the behavior of different membranes during long-term operation. On the light of the results obtained previously in the present study, the experiments were carried out at a TMP of 2.0 bar and a temperature of 70 ^{o}C, where at these conditions the highest flux was obtained. The feed was changed at regular intervals, where the module was completely drained off the old feed every 90 min of operation and the experiment was continued with a fresh batch of limed juice, prepared appropriately.

No module cleaning was performed between feed changes. Two different types of membrane were tested simultaneously. Samples of MF and UF permeate and the retentate were taken at the end of the experiments only (after 1.5 hour) to explore the effects of the operating time on the microfiltration and ultrafiltration processes. The experiment was conducted in a batch mode with permeate and retentate recycle.

Figure 10 shows that the permeate flux during the course of the operation for the GRM0.1PP MF and GR40PP UF membranes. Each data point represents the average flux obtained in one production cycle (during the 90 min).

From the results shown in Fig. 10, it is clear that the flux of both GRM0.1PP MF and GR40PP UF membranes display an exponential decrease with time and the flux of GRM0.1PP MF membrane was higher than that of the flux of GR40PP UF

membrane. The average flux of GRM0.1PP MF at beginning of the trials is about 160 L/m^2.h. The value decreased progressively and reached a value of about 81 L/m^2.h after 7.5 hours of operation. The flux of GR40PP UF decreased from about 130 L/m^2.h to 59 L/m^2.h after 7.5 hours of operation.

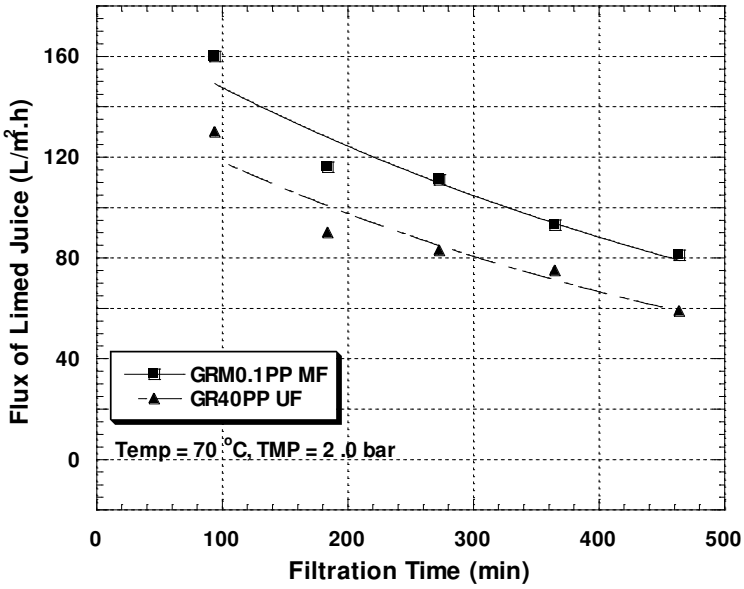

Figure 10: Flux of limed juice versus operating time for GRM0.1PP MF and GR40PP UF at temperature of 70 °C and TMP of 2.0 bar.

Figure 11 shows the permeate flux of the GRM0.2PP MF and GR60PP UF membranes during continuous operation of 6 hours. The flux exhibits exponential decline with time for both and is nearly independent of the membrane type until 180 min of operation. The curves diverge after about 180 min. The flux decline is fully understood as a result of foulants deposition on the bare membrane. This deposition is assumed to be at least partially permeable to fluid flow in the beginning i.e., there is a small finite flow through even the blocked pores. As the membrane surface becomes more heavily fouled, the fouling material will also begin to deposit on the fouling layer causing an increase in the hydraulic resistance which diminished the permeate flux.

5. CONCLUSIONS AND RECOMMENDATIONS

This work presents an on-site assessment of polymeric membrane plate modules for microfiltration and ultrafiltration of sugarcane juice on a laboratory-scale level to examine the flux decline of membrane. A test rig employs a DSS Labstak® M10 module was designed and constructed at the Sugar Technology Research Institute. Trials were done in Qus pilot plant at Qus Sugar Mill, Qena, Egypt using a fresh mixed juice. Moreover, a numerical model which uses the two-dimensional convective-diffusion equation was proposed and used to predict the permeate flux decline during MF and UF filtration of sugarcane juice.

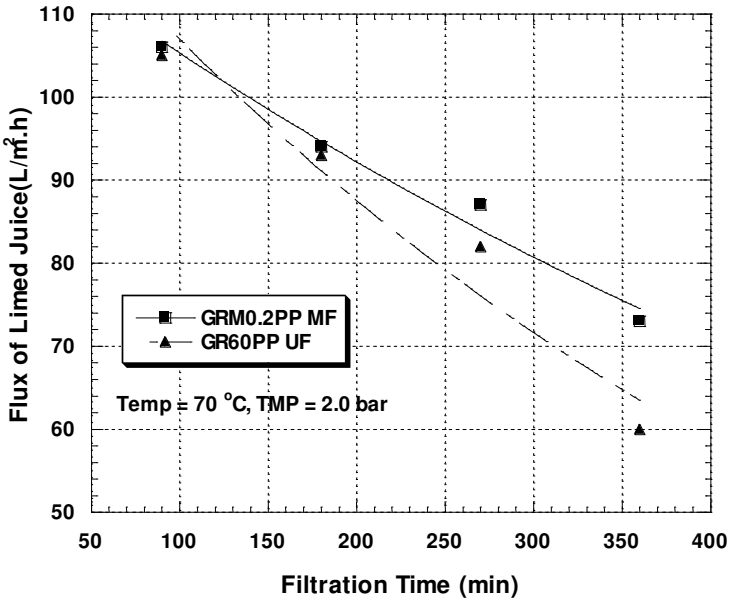

Figure 11: Flux of limed juice versus operating time for GRM0.2PP MF and GR60PP UF at temperature of 70 °C and TMP of 2.0 bar.

In this paper, the effects of different parameters on the behavior of three membranes, one microfiltration membrane (GRM0.1pp) and two ultrafiltration membrane (GR40pp, and GR60pp) for filtering both mixed juice and clear juice were studied experimentally and numerically. It was noticed that in all cases the membrane fouling was the highest at the first period of operation. This could be attributed to the formation of a concentration polarization layer. Temperature has a remarkable effect on the permeate flux. Increasing transmembrane pressure within the examined range did not causes flux decline. The numerical results of the permeate flux decline obtained in this study agree well with their experimental counterparts. The present study found that the proper choice of membrane is GR40pp (100 KD MWCO) as it gives permeate with high quality and reasonable flux.

REFERENCES

1. Balakrishnan M., Dua M., and Bhagat J.J., Effect of operating parameters on sugarcane juice ultrafiltration: results of a field experience. Separation and Purification Technology, 19 (2000) 209–220.
2. Madsen R.F., Nielsen W.K., and Kristensen S., Purifying sugar juice. GB Patent, No. 2090861 A (1982).
3. Song L., Flux decline in crossflow microfiltration and ultrafiltration: mechanisms and modeling of membrane fouling. Journal of Membrane Science, 139 (1998) 183–200.
4. Song L., and Elimelech M., Theory of concentration polarization in crossflow filtration, J. Chem. Soc., Faraday Trans., 91 (1995) 3389-3398.

5. Makardij A.A., Farid M.M., and Chen X.D., A simple and effective model for cross-flow microfiltration and ultrafiltration, Can. J. Chem. Eng., 80 (2002) 28–36.
6. Wang S.M., Liu S.X., Wang Z., Lv Y.W., and Liu X.C., Study of hydrodynamics character when permeating soy by hollow-fiber microfiltration membrane module, J. Membr. Sci. Tech. (China), 22 (2002) 6–11.
7. Mohammadi T., Kazemimoghadam M., and Saadabadi M., Modeling of membrane fouling and flux decline in reverse osmosis during separation of oil in water emulsions, Desalination, 157 (2003) 369-375.
8. Vincent M. C., Bergantinos E., Alvarez S., and Lora J., Ultrafiltration permeate flux decline prediction for gel layer forming solutes using monotubular ceramic membranes, Desalination, 240 (2009) 89-93.
9. Ho-Ming Yeh, Decline of permeate flux for ultrafiltration along membrane tubes, Desalination, 145 (2002) 153-l 57.
10. Shon H.K., Vigneswaran S., Kandasamy J., and Shim W.G., Ultraflitration of wastewater with pretreatment: evaluation of flux decline models, Desalination 231 (2008) 332–339.
11. Vassilieff C.S., Doneva T.A., and Ljutov L.G., Crossflow microfiltration of bentonite-in-water dispersions: Initial transient effects at low concentration, J. Membr. Sci., 119 (1996) 65–80.
12. Mikulasek P., Dolecek P., Smidova D., and Pospisil P., Crossflow microfiltration of mineral dispersions using ceramic membranes, Desalination, 163 (2004) 333-343
13. Che-Jen Lin, Pritesh Rao, and Saqib Shirazi, Effect of operating parameters on permeate flux decline caused by cake formation: a model study, Desalination, 171 (2004) 95-105.
14. Mohammadi T., Kohpeyma A., and Sadrzadeh M., Mathematical modeling of flux decline in ultrafiltration, Desalination, 184 (2005) 367–375.
15. Furukawa T., Kokubo K., Nakamura K., and Matsumoto K., Modeling of the permeate flux decline during MF and UF cross-flow filtration of soy sauce lees, Journal of Membrane Science, 322 (2008) 491–502.
16. Shengji X., Juanjuan Y., and Naiyun G., An empirical model for membrane flux prediction in ultrafiltration of surface water, Desalination, 221 (2008) 370–375.
17. Wang Z., Chu J., Wub W., and Yao J., Study of unsteady-state flux prediction in cross-flow microfiltration, Desalination, 238 (2009) 290–301.
18. Lee Y., and Clark M.M., Modeling of flux decline during crossflow ultrafiltration of colloidal suspensions, Journal of Membrane Science 149 (1998) 181-202.
19. Geraldes V., Semião V., and Pinho M.N. de, Flow and mass transfer modeling of nanofiltration, Journal of Membrane Science, 191 (2001) 109-128.
20. Ali K. Abdel-Rahman, Abbara A.A., and Bayoumi M.R., Numerical modeling of concentration profiles in membrane channel, Journal of Engineering Science, Faculty of Engineering, Assiut University, 34 (2006) 251-274.
21. Madireddi K., Babcock R.B, Levine B., Kim J.H., and Stenstrom M.K., An unsteady-state model to predict concentration polarization in commercial spiral wound membranes, Journal of Membrane Science, 157 (1999) 13-34.

22. Ali K. Abdel-Rahman, Numerical modeling of concentration polarization in reverse osmosis desalination system, Journal of Engineering Science, Faculty of Engineering, Assiut University, 36 (2008) 87-104.
23. Pak A., Mohammadi T., Hosseinalipour S.M., and Allahdini V., CFD modeling of porous membranes, Desalination, 222 (2008) 482–488.
24. Anderson D.A., Tannehill J.C., and Pletcher R.H., Computational fluid mechanics and heat transfer, Hemisphere Publishing Corporation, New-York (1984).
25. Patankar S.V. and Spalding D.B., A calculation procedure for heat, mass and momentum transfer in three-dimensional parabolic flows. International Journal of Mass and Heat Transfer, 15 (1972) 1787-1806.
26. Ali K. Abdel-Rahman, and Suzuki K., Laminar channel flow with fluid injection accounting for the flow in the porous wall, Proceedings of the 5th Int. Conference of Fluid Mechanics, Cairo, (1995) 367-379.
27. Geraldes V., Semião V. and Pinho M.N. de, Numerical modeling of mass transfer in slits with semi-permeable membrane walls. Engineering Computations, 17 (2000) 192-217.
28. Ali K. Abdel-Rahman, Flow and heat transfer characteristics of internal flows with fluid injection, PhD thesis, Kyoto University, Kyoto, Japan (1992).
29. Brian P.L.T., Concentration polarization in reverse osmosis desalination with variable flux and incomplete salt rejection, Ind. Eng. Chem. Fund., 4 (1965) 439-445.
30. Wiley D.E. and Fletcher D.F., Techniques for computational fluid dynamics modeling of flow in membrane channels, Journal of Membrane Science, 211 (2003) 127–137.
31. Berman A.S., Laminar flow in channels with porous walls, Journal of Applied Physics, 24 (1953) 1232-1235.
32. Bubnic Z., Kadlec P., Urban D. and Bruhns M., Sugar technologists' manual-chemical and physical data for sugar manufactures and users, Bartens, Berlin, Germany (1995).
33. Abbara A.A., Study of using membrane filtration in clarification of sugar juices, PhD Thesis, Sugar Technology Research Institute, Assiut University, Assiut, Egypt (2005).

نمذجة اضمحلال تدفق العصير المستخلص خلال الترشيح الميكروسكوبي والترشيح الفائق العرضي لعصير قصب السكر

د. على كامل عبد الرحمن ، د. عبد العزيز عبارة و أ.د. محمد رجب بيومي

ملخص – النتائج العملية لظاهرة اضمحلال تدفق العصير المستخلص مع الزمن من خلال تجارب الترشيح الميكروسكوبى والترشيح الفائق تم مقارنتها مع نظيراتها التي تم التنبؤ بها عدديا باستخدام معادلات الحمل–الانتشار ثنائية الأبعاد. المحاكاة العددية لانتقال السريان والحرارة تمت باستخدام معادلات كمية الحركة والطاقة ثنائية الأبعاد. نوعان مختلفان من عصائر قصب السكر هما العصير الرائق والعصير الخليط المعالج لأس هيدروجيني 7.5 تم اختبارهما فى هذه الدراسة. التجارب العملية اجريت باستخدام خلية مسطحة ذات سريان عرضى تستخدم ثلاثة أنواع مختلفة من أغشية الترشيح الميكروسكوبى والترشيح الفائق المصنعة من "البوليسلفون" (حد القطع للوزن الجزيئى: 1 ميكرون، 25 و100 كيلودالتون). تمت دراسة تأثير متغيرات العمليات المختلفة مثل ضغط الأغشية (عند ضغوط: 1، 1.5 و2 بار) ودرجة حرارة التغذية (درجات الحرارة: 50، 60 و 70 درجة مئوية) على تدفق العصير المستخلص.

أظهرت الدراسة الحالية ان تدفق العصير المستخلص الذي تم الحصول عليه عمليا وعدديا يزداد مع زيادة ضغط الاغشية فى جميع الاغشية التى استخدمت فى هذه الدراسة . أضافة الى ذلك ، فإن التدفق ازداد مع زيادة درجة حرارة عصير التغذية ويتناقص مع الزمن. القيم العددية لتدفق العصير المستخلص اظهرت تطابقا جيدا مع نظيراتها العملية.